

Electrochemical immunoassay for the prostate specific antigen using a reduced graphene oxide functionalized with a high molecular-weight silk peptide

Yanying Wang^{1,2} · Ying Qu¹ · Guishen Liu³ · Xiaodong Hou³ · Yina Huang³ · Wangze Wu⁴ · Kangbing Wu² · Chunya Li¹

Received: 19 March 2015 / Accepted: 19 June 2015 / Published online: 1 July 2015
© Springer-Verlag Wien 2015

Abstract High molecular-weight silk peptide (SP) was used to functionalize the surface of nanosheets of reduced graphene oxide (rGO). The SP-rGO nanocomposite was then mixed with mouse anti-human prostate specific antigen monoclonal antibody (anti-PSA) and coated onto a glassy carbon electrode to fabricate an immunosensor. By using the hexacyanoferrate redox system as electroactive probe, the immunosensor was characterized by voltammetry and electrochemical impedance spectroscopy. The peak current, measured at the potential of 0.24 V (vs. SCE), is distinctly reduced after binding prostate specific antigen (PSA). Response (measured by differential pulse voltammetry) is linearly related to PSA concentration in the range from 0.1 to 5.0 ng·mL⁻¹ and from 5.0 to 80.0 ng·mL⁻¹, and the detection limit is 53 pg·mL⁻¹ (at an SNR of 3). The immunosensor was successfully applied to the determination of PSA in clinical serum samples, and the

results were found to agree well with those obtained with an enzyme-linked immunosorbent assay.

Keywords Silk peptide · Reduced graphene oxide · Immunosensor · Prostate specific antigen · Electrochemistry

Introduction

Prostate specific antigen (PSA) is an important biomarker highly related to diagnosis, prevention, and treatment of prostate tumor [1, 2]. High PSA concentration in serum means a potential risk in suffering from prostate cancer [3]. The typical PSA cutoff level in serum regarding to suspicious prostate cancer is 4 ng·mL⁻¹ [4]. To monitor PSA level in physiological fluids is essential for the early diagnosis and the accurate evaluation of a drug therapy. Traditional assay methods such as enzyme-linked immunosorbent assay (ELISA) [5], radioimmunoassay [6], fluorescence immunoassay [7], mass spectrometric immunoassay [8], and immune-polymerase chain reaction assay [9] have their own disadvantages and limitations unavoidably, resulting in an increasing demand for simple, sensitive and easily automated devices. Electrochemical immunosensor is considered to be an outstanding alternative and has been widely applied for clinical diagnosis [10–12]. In order to improve the sensitivity toward PSA, many nanomaterials based on metal nanoparticles, carbon nanotubes, reduced graphene oxide nanosheets and their composites have been used as sensing platform to immobilize anti-PSA [13–21].

Carbon nanotubes and graphene nanosheets possess some extraordinary properties including superior electrical conductivity, high thermal conductivity, good electron field emitters, high specific surface area and excellent mechanical properties [22–24]. The key challenge in harnessing of these unique properties is the difficulty of reliable manipulation of well-

Electronic supplementary material The online version of this article (doi:10.1007/s00604-015-1552-2) contains supplementary material, which is available to authorized users.

✉ Kangbing Wu
kbwu@mail.hust.edu.cn

✉ Chunya Li
lcychem@yahoo.com

¹ Key Laboratory of Analytical Chemistry of the State Ethnic Affairs Commission, College of Chemistry and Materials Science, South-Central University for Nationalities, Wuhan 430074, China

² Key Laboratory for Large-Format Battery Materials and System, Ministry of Education, School of Chemistry and Chemical Engineering, Huazhong University of Science and Technology, Wuhan 430074, China

³ Chaozhou Quality and Measurement Supervision and Inspection Institute, Chaozhou 521011, China

⁴ The central hospital of Wuhan, Wuhan 430014, China

dispersed carbon nanotubes and graphene nanosheets. Chemical and physical functionalization of graphene has become a focus of especial interest, because they can not only stabilize, but also induce new properties [25]. The covalent modification has been demonstrated a worthwhile method for fabricating functionalized reduced graphene oxide nanosheets. The graphene oxide nanosheets can supply many active sites, e.g., epoxy groups, for the reacting with modifiers such as amines, amino acids, ionic liquids and biomolecules [26, 27]. High molecular-weight silk peptide, a partly hydrolysis product of silk protein, has also been used as a functional monomer to modify the reduced graphene oxide nanosheets. The obtained nanocomposite has been demonstrated to be an enhanced element for the amperometric sensing of phenolic compounds based on the catalytic properties of tyrosinase [28].

Herein, the SP-rGO nanocomposites were used as a sensing platform to construct an electrochemical immunosensor for PSA. High molecular-weight silk peptide not only provides abundant active groups, mainly amino groups and carboxyl groups, for the immobilization of anti-PSA, but also forms a biocompatible microenvironment that is helpful for maintaining the bioactivity of anti-PSA. In addition, the reduced graphene oxide nanosheets possess large surface area and high conductivity. Therefore, SP-rGO nanocomposites will not only promote more anti-PSA to be loaded on, but also improve the electrochemical response of potassium ferricyanide, thus accordingly enhance the sensitivity of the developed immunosensor. Voltammetry and electrochemical impedance techniques were used to characterize the immunosensor. Experimental conditions for PSA determination were optimized. Furthermore, practical application of the immunosensor for PSA determination in clinical serum samples was evaluated.

Experimental

Chemicals and apparatus

High molecular-weight silk peptide (SP, MW=10,000–15,000 Da) was bought from Huzhou Xintiansi Biotech Co., Ltd (<http://www.chinatiansi.com/en/index.htm>). Mouse anti-human PSA monoclonal antibody (anti-PSA), prostate specific antigen (PSA), α -fetoprotein, and human IgG were purchased from Beijing Biosynthesis Biotechnology Co., LTD (<http://www.bioss.com.cn>). Specpure graphite, glutaraldehyde, and bovine serum albumin (BSA) were purchased from Sinopharm Chemical Reagent Co., Ltd. (<http://www.sinoreagent.com>). Other chemicals were analytical grade and were used as received. All of the solutions were prepared with ultrapure water. Experiments were carried out at room temperature without other statements.

Electrochemical measurements were performed with CHI 660 C electrochemical workstation (<http://www.chinstr.com>). A conventional three-electrode system consists of an immunosensor as the working electrode (3 mm in diameter, <http://www.gaossunion.com>), a Pt wire as auxiliary electrode, and a saturated calomel reference electrode (SCE). JSM-6700 F field emission scanning electron microscopy (<http://www.jeol.co.jp/en>) was applied to the electrode surface analysis. Transmission electron microscopy (TEM) images were obtained on a FEI Tecnai G2 20S-TWIN instrument (<http://www.fei.com/products/tem/tecnai>) operating at an acceleration voltage of 200 kV. X-ray photoelectron spectroscopy (<http://www.thermoscientific.com>) was used to analysis of the composition of nanocomposites. X-ray diffraction was conducted on D8 Advanced X-ray diffractometer (<http://www.bruker.com>). FTIR was recorded on a FTIR-8700 infrared spectrophotometer (<http://www.shimadzu.com>). Raman spectra were performed on a LabRAM HR800 confocal Raman microscopy system (<http://www.horiba.com>) using 532 nm laser.

Synthesis of SP-rGO nanosheets

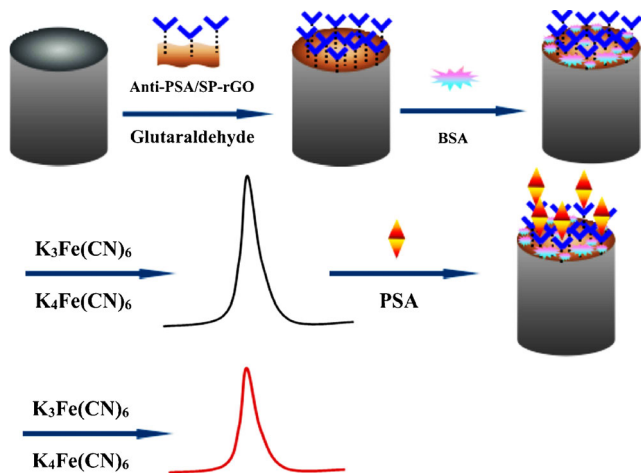
Graphite oxide was synthesized using the Hummers method with some modifications [29, 30]. The graphite powder (10 g) was loaded into a mixed solution containing concentrated H_2SO_4 (15 mL), $\text{K}_2\text{S}_2\text{O}_8$ (5 g), and P_2O_5 (5 g), and was heated to 80 °C. The resultant dark blue mixture was thermally isolated and allowed to cool to room temperature. The mixture was then carefully diluted with distilled water, filtered, and washed until the rinse water became neutral. The product was dried at ambient temperature overnight. Concentrated H_2SO_4 (17 mL) was added to the mixture of pre-oxidized graphite powder (0.5 g) and KNO_3 (0.45 g). KMnO_4 (2.25 g) was added gradually with stirring and cooling, and kept at 0 °C for 2 h. Then, the mixture was stirred at room temperature for 5 days. The reaction was terminated by the addition of 50 mL of a mixed solution containing H_2SO_4 (3 %) and H_2O_2 (0.5 %). The mixture was washed with ultrapure water until the rinse water became neutral. After that, the graphite oxide was dispersed into water and was subjected to dialysis for one week. Then, ultrasonication was used to exfoliate graphene oxide nanosheets from the graphite oxide surface. Subsequently, the unexfoliated graphite oxide was removed from the system using centrifugation [31]. The solution was evaporated to afford graphene oxide nanosheets.

The procedure for the SP-rGO nanosheets preparation was briefly described as following [28]: 4.0 mg of the graphene oxide nanosheets, 20.0 mg of high molecular-weight silk peptide and 16.0 mg of KOH were added into ultrapure water (20.0 mL), and were vigorously stirred to obtain a homogeneous mixture. The mixture was kept at 80 °C for 24 h. After being cooled to room temperature, 2.0 mL NaBH_4 solution

(1.0 mol L^{-1}) was added to reduce the graphene oxide nanosheets. The reaction was kept at $80 \text{ }^\circ\text{C}$ for 2 h. Centrifugation was used to separate SP-rGO nanosheets with thorough washing. The obtained SP-rGO nanocomposites were characterized with TEM, XRD, XPS, FTIR and Raman spectroscopy. All results were shown in Fig. S1 – S5 (Electronic Supplementary Material), and confirmed the successful modification of SP on the reduced graphene oxide nanosheets surface.

Fabrication of PSA immunosensor

Prior to modification, glassy carbon electrodes were polished with emery paper and alumina slurries. The electrodes were successively ultrasonicated in nitric acid, ethanol, and water, and then allowed to dry at room temperature. The SP-rGO nanocomposites ($25 \text{ } \mu\text{L}$, 2 mg mL^{-1}) and anti-PSA ($10 \text{ } \mu\text{L}$, $5 \text{ } \mu\text{g mL}^{-1}$) were homogeneously dispersed in phosphate buffer. In subsequent steps, the mixed solution was drop coated onto the cleared glassy carbon electrode surface and dried at $4 \text{ }^\circ\text{C}$. Then, the anti-PSA/SP-rGO composite film electrode was treated with glutaraldehyde vapor for 5 min to stabilize anti-PSA via a cross-linking reaction. After that, the modified electrode was incubated in a bovine serum albumin solution to block all unspecific sites to produce an immunosensor that was denoted as anti-PSA(BSA)-SP-rGO/GCE. The obtained immunosensor was fully washed with ultrapure water to remove all chemicals that were physically adsorbed. When being used for immunosensing, anti-PSA(BSA)-SP-rGO/GCE was incubated in a PSA solution for 30 min, and was washed thoroughly with phosphate buffer. Based on specific binding between anti-PSA and PSA, the immunosensor can selectively recognize PSA and give corresponding electrochemical signals using $\text{K}_3[\text{Fe}(\text{CN})_6]/\text{K}_4[\text{Fe}(\text{CN})_6]$ as electroactive probes. The fabrication procedure and electrochemical response mechanism of the immunosensor were presented in Scheme 1.



Scheme 1 Schematic for the fabrication and electrochemical response of the PSA immunosensor

Electrochemical measurements

Cyclic voltammetric and differential pulse voltammetric measurements were carried out in an electrochemical cell containing $5.0 \text{ mM K}_3[\text{Fe}(\text{CN})_6]/\text{K}_4[\text{Fe}(\text{CN})_6]$ (1:1), 0.1 M KCl and 0.01 M phosphate buffer. The current difference between the electrochemical response of the immunosensor before and after being interacted with PSA was used as a quantitative standard to evaluate its sensing performance. The pulse amplitude, pulse period, and pulse width of differential pulse voltammetry were 50 mV , 0.2 s , and 50 ms , respectively. Electrochemical impedance spectroscopy was carried out in the frequency range from 1.0×10^5 to 0.1 Hz .

ELISA assay

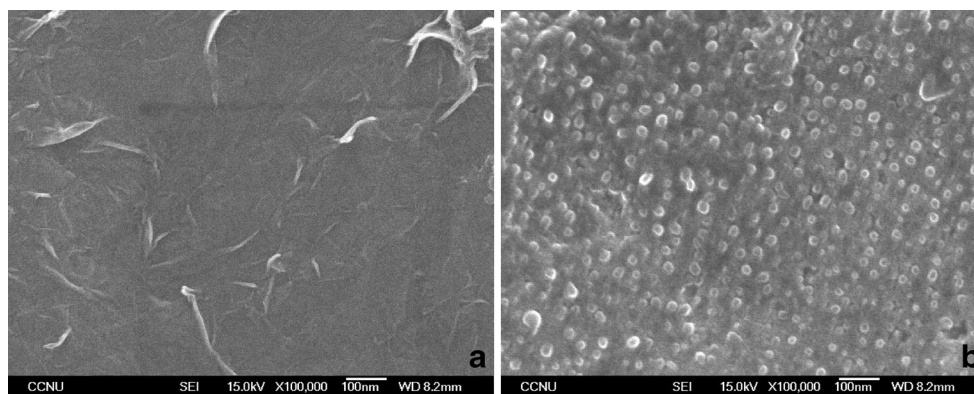
Clinic serum sample was kindly supplied by the Central Hospital of Wuhan (<http://www.zxhospital.com>). The blood serum sample was simply diluted with phosphate buffer, and was measured using the developed immunosensor. Enzyme-linked immunosorbent assays were performed using commercial kits (<http://www.leadmanbio.com>) according to the manufacturer's instructions, and were detected using Olympus AU5421 automatic biochemical analyzer (<http://www.olympus-global.com/en>).

Results and discussion

Characterization of PSA immunosensor

To successfully fabricate the SP-rGO-based immunosensor, the stabilized modification of the SP-rGO nanosheets and the anti-PSA(BSA)-SP-rGO composites on glassy carbon electrode surface were very crucial. Hydrophobic interaction and π - π interaction between the rGO nanosheets and the glassy carbon electrode surface will be beneficial to the stabilization of these nanocomposites. In addition, the covalent cross-linking reaction between amino groups, which exist in anti-PSA and SP, and aldehyde groups come from glutaraldehyde are great helpful to immobilize anti-PSA onto the sensing platform. Figure 1 shows the scanning electron microscopic images of the SP-rGO/GCE (a) and the anti-PSA(BSA)-SP-rGO/GCE (b), respectively. It is obvious that the SP-rGO nanosheets modified electrode displayed tiny wrinkles over the whole surface with mountainous peaks. The overlap of the SP-rGO nanosheets with two or more layers can be clearly observed. Scanning electron microscopic image of the anti-PSA(BSA)-SP-rGO/GCE reveals that some nanoparticles were homogeneously distributed onto the electrode surface. The morphologic difference between the SP-rGO/GCE and the anti-PSA(BSA)-SP-rGO/GCE is mainly caused by the

Fig. 1 Scanning electron microscopic images of the SP-rGO/GCE (a) and the anti-PSA(BSA)-SP-rGO/GCE (b)



immobilization of anti-PSA, thus meaning the successful fabrication of the immunosensor.

Electrochemical impedance spectroscopy is an effective technique to explore the interfacial information of the modified electrode during the stepwise assembled processes. The Nyquist plot commonly includes a semicircular portion and a linear portion. The semicircle portion at higher frequencies is corresponding to the electron-transfer limited process, and the linear part at lower frequencies is attributed to the diffusion process. The semicircle diameter corresponds to the charge transfer resistance (R_{et}). $K_3[Fe(CN)_6]/K_4[Fe(CN)_6]$ were used as electroactive probes to study the charge transfer resistance (R_{et}) of the bare glassy carbon electrode (a), the SP-rGO/GCE (b), the anti-PSA-SP-rGO/GCE (c), the anti-PSA(BSA)-SP-rGO/GCE (d) and the PSA-anti-PSA(BSA)-SP-rGO/GCE (e), respectively. The corresponding Nyquist plots were shown in Fig. 2a. The Randles equivalent circuit, which was inserted in Fig. 2a, was further chosen to fit the impedance data obtained in the experiments using ZSIMPWIN300 software, where R_s is the uncompensated solution resistance, Q is the constant phase element, R_{et} is the charge transfer resistance, Z_w is the Warburg impedance. From curve a to e, the fitted values of R_{et} for $K_3Fe(CN)_6/K_4Fe(CN)_6$ at these electrodes are 133.8, 332.7, 696, 1664, and 2439 ohm, respectively. Correspondingly, the average value for three independent measurements are calculated to be 133.6 ohm (SD=4.3 %), 333.1 ohm (SD=4.5 %), 694.5 ohm (SD=3.8 %), 1664.8 ohm (SD=3.3 %), and 2438.3 ohm (SD=2.8 %). It was obvious to see that R_{et} for the bare GCE (curve a) is less than the electrode modified with SP-rGO nanosheets (curve b). The main reason can be ascribed to the poor conductivity of high molecular-weight silk peptide. The R_{et} value significantly increased after immobilizing anti-PSA through the cross-linking reaction with glutaraldehyde (curve c). When all unspecific sites were blocked with bovine serum albumin, the charge transfer resistance was further enhanced (curve d), meaning the successful reaction between BSA and the remained aldehyde groups. In the following step, the fabricated immunosensor was incubated in a PSA solution. Immunoreaction between PSA and the

immobilized anti-PSA leads to the further increasing of charge transfer resistance of $K_3Fe(CN)_6/K_4Fe(CN)_6$ (curve e).

Figure 2b presents the cyclic voltammograms of 5.0 mM $K_3Fe(CN)_6/K_4Fe(CN)_6$ at the bare glassy carbon electrode (a), the SP-rGO/GCE (b), the anti-PSA-SP-rGO/GCE (c), the anti-PSA(BSA)-SP-rGO/GCE (d) and the PSA-anti-PSA(BSA)-SP-rGO/GCE (e). It is obvious to see that the redox peak current gradually decreased with the fabricating procedure being successively performed. The oxidation peak current, shown in Fig. 2b, was used to calculate the electrically active surface area according the following equation: $ip = 2.69 \times 10^5 n^{3/2} AD^{1/2} cv^{1/2}$. Where, n is the electron transfer number for the oxidation of $K_4Fe(CN)_6$; the coefficient of diffusion (D) for $K_4[Fe(CN)_6]$ in 0.1 M KCl is $0.65 \times 10^{-5} \text{ cm}^2 \cdot \text{s}^{-1}$; the concentration (c) of $K_4[Fe(CN)_6]$ is $5 \times 10^{-3} \text{ M}$; scan rate (v) is $0.1 \text{ V} \cdot \text{s}^{-1}$. Subsequently, the current density (j) was also calculated and presented in Fig. 2c. The calculated electrically active surface area gradually declined from a to e, leading the current density increased accordingly. It is notable that a significant increase was observed after the anti-PSA(BSA)-SP-rGO/GCE has been incubated in a PSA solution ($50 \text{ ng} \cdot \text{mL}^{-1}$). This phenomenon is well consistent with the result from electrochemical impedance spectroscopy. The significant variation of electrochemical signal during the incubation process not only indicated that an immunoreaction has occurred between PSA and the anti-PSA(BSA)-SP-rGO/GCE, but also suggested a high sensitivity of the developed immunosensor.

Optimization of experimental conditions

The following parameters were optimized: (a) Sample pH value; (b) incubation temperature; (c) incubation time. Respective data are given in the Electronic Supporting Material as Fig. S 6. The following experimental conditions were found to give best results: (a) A sample pH value of 6.0; (b) an incubation temperature of $35 \text{ }^\circ\text{C}$; and (c) an incubation time of 30 min.

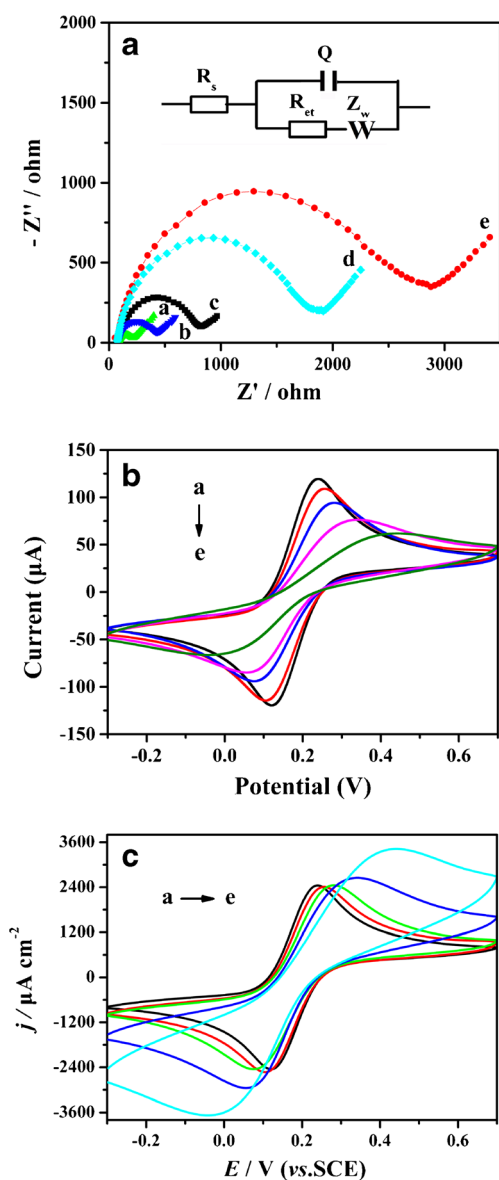


Fig. 2 Nyquist plots (a) and cyclic voltammograms (b and c) of 5.0 mM $K_3[Fe(CN)_6]/K_4[Fe(CN)_6]$ (1:1) at the bare glassy carbon electrode (a), the SP-rGO/GCE (b), the anti-PSA-SP-rGO/GCE (c), the anti-PSA(BSA)-SP-rGO/GCE (d) and the PSA-anti-PSA(BSA)-SP-rGO/GCE (e). Supporting electrolyte solution: 0.01 M phosphate buffer (pH 6.0)+0.1 M KCl solution; Scan rate: 100 mV·s⁻¹

Stability and reproducibility

The storage stability of the immunosensor was investigated by comparing the peak current response of PSA at the concentration of 50.0 ng·mL⁻¹. After being stored in a refrigerator for six weeks, the immunosensor retains about 95 % of its original response, meaning good storage stability. The reproducibility for the PSA determination was evaluated by measuring $K_3(FeCN)_6/K_4(FeCN)_6$ (5.0 mM) with six independently prepared immunosensors. The calculated RSD, 4.15 %, indicates reliable fabrication reproducibility. After being regenerated in

a glycine hydrochloric acid buffer (0.2 M, pH 2.8), the immunosensor was used for determining PSA (50.0 ng·mL⁻¹) repeatedly. A RSD value of 4.04 % was obtained for the six independent determinations, meaning no perceivable influence on the biosensing performance during the regeneration process.

Selectivity of the immunosensor

The specificity of the immunosensor plays an important role in the biological assay without separation. Selectivity of the immunosensor was evaluated by determining PSA in the presence of some potentially interfering species. After being incubated in a PSA solution (10.0 ng·mL⁻¹) for 30 min, the current response of the immunosensor was presented in Fig. S 7 (a). With the identical procedure, the current response of a PSA solution (10.0 ng·mL⁻¹) containing alpha-fetoprotein (100.0 ng·mL⁻¹), human IgG (100.0 ng·mL⁻¹), BSA (1.0 µg·mL⁻¹), Vc (1.0 µg·mL⁻¹), L-Cysteine (1.0 µg·mL⁻¹) and L-Lysine (1.0 µg·mL⁻¹) was also measured using the immunosensor, and was shown in Fig. S 7 (b). It was found that these potentially interfering species had almost no influence on the current response of PSA (signal change below 5 %), indicating that the immunosensor possesses excellent selectivity towards PSA.

Analytical characteristics

The analytical performance of the immunosensor was explored by quantifying the PSA standard solution according to the above-described procedure. The typical differential pulse voltammograms at different concentrations are presented in Fig. 3a. It was found that the peak current of $K_3(FeCN)_6/K_4(FeCN)_6$ decreased with the PSA concentration increasing. As shown in Fig. 3b, a good linear relationship between the peak current variation (ΔI) and PSA concentration (c) was obtained in the range of 0.1~5.0 ng·mL⁻¹ and 5.0~80.0 ng·mL⁻¹. At high PSA concentration, the ΔI values would tend to be stable due to the saturation binding of PSA to the immobilized anti-PSA. The equations can be expressed as following: $\Delta I (\mu A) = 2.14 c (\text{ng} \cdot \text{mL}^{-1}) + 9.75$ ($R = 0.990$) and $\Delta I (\mu A) = 0.175 c (\text{ng} \cdot \text{mL}^{-1}) + 19.4$ ($R = 0.994$). The detection limit is calculated to be 0.053 ng·mL⁻¹ ($S/N = 3$). The calibration curves present two slopes, meaning different sensitivity towards the voltammetric determination of PSA. The difference may come from the restricted amount of anti-PSA immobilized on the SP-rGO/GCE surface [14, 15]. During the incubation process, PSA selectively interacted with the active sites of anti-PSA. As the PSA concentration is low, the active sites are abundant for PSA binding, thus showing a high sensitivity. With the PSA concentration increasing, the amount of active sites becomes relatively small. As a result, the sensitivity of the immunosensor declines accordingly. The sensing

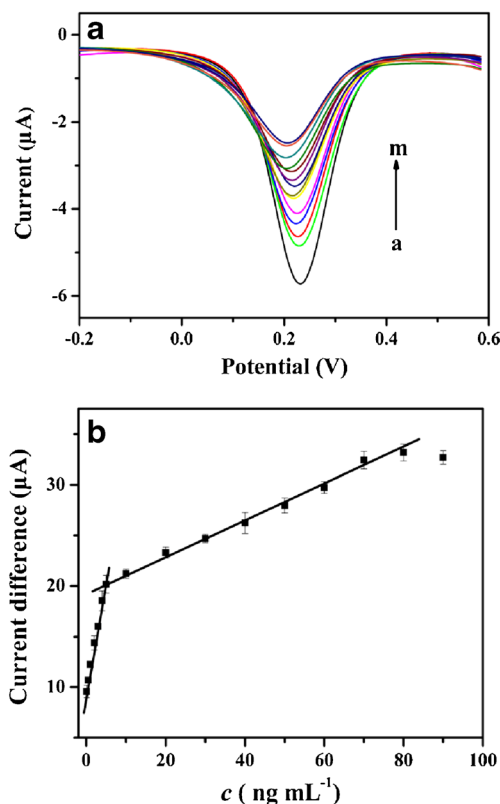


Fig. 3 **a** Differential pulse voltammograms of 5.0 mM $K_3[Fe(CN)_6]/K_4[Fe(CN)_6]$ (1:1) at the immunosensor after being incubated into PSA solution at different concentration (Form a to m: 0.1, 0.5, 1.0, 2.0, 3.0, 4.0, 5.0, 10, 20, 30, 40, 50, 60, 70, 80 $ng \cdot mL^{-1}$); **b** Calibration curve for PSA determination

performance of the developed immunosensor was compared with the previously reported immunosensors for PSA. As shown in Table S1 in Supporting Information, the immunosensor fabricated with the SP-rGO nanosheets exhibits a wider linear range and a lower detection limit than some of them. The immunosensor also has the merits of simple, rapidness, and high selectivity for the PSA determination. Thus, it should possess a promising application in real sample analysis.

Analysis of PSA in clinical serum samples

The applicability of the developed immunosensor was evaluated by determining PSA in serum samples. The results were compared with those obtained using commercial ELISA Kits. On the basis of these data summarized in Table 1, it was found that no significant difference can be observed between the immunosensor and the ELISA method, demonstrating a high accuracy for the PSA determination. The developed immunosensor can be considered as a versatile, reliable and accurate tool for screening of PSA in clinical samples.

Table 1 Determination of PSA in clinical serum sample ($n=5$)

Serum sample	This method ($ng \cdot mL^{-1}$)	Average ($ng \cdot mL^{-1}$)	RSD (%)	ELISA ($ng \cdot mL^{-1}$)	RD ^a (%)
1	0.1386	0.1433	2.78	0.1435	0.07
	0.1451				
	0.1445				
	0.1484				
	0.1400				
2	3.231	3.197	2.43	3.264	1.04
	3.145				
	3.089				
	3.246				
	3.276				
3	12.54	12.22	1.55	12.45	0.93
	12.38				
	12.16				
	12.11				
	12.28				

^a RD means the relative deviation between the average value and the ELISA result

Conclusions

The integration of high molecular-weight silk peptide with the reduced graphene oxide nanosheets provided some profitable characteristics such as high specific surface area, excellent conductivity, and abundant active sites for further modification, leading the anti-PSA amount loaded on the electrode surface increasing. An immunosensor based on the SP-rGO composites was thus fabricated for the determination of PSA. The results indicated that the immunosensor can be used to determine PSA with high sensitivity, good selectivity and excellent accuracy. The practicability of the immunosensor has also been demonstrated by determining PSA in clinical serum samples. We anticipate that SP-rGO nanocomposite based immunosensors can be expanded rapidly for other tumor markers.

Acknowledgments The authors gratefully acknowledge the financial supports from National Natural Science Foundation of China (No. 21275166), China Scholarship Council (No. 201307780006), and Research Foundation of General Administration of Quality Supervision, Inspection and Quarantine of the People's Republic of China (No. 2013Qk286).

References

1. Stamey TA, Yang N, Hay AR, McNeal JE, Freiha FS, Redwine E (1987) Prostate-specific antigen as a serum marker for adenocarcinoma of the prostate. *New Engl J Med* 317:909
2. Catalona WJ, Richie JP, Ahmann FR, Hudson MA, Scardino PT, Flanigan RC, deKemion JB, Ratliff TL, Kavoussi LR, Dalkin BL (1994) Comparison of digital rectal examination and serum prostate

- specific antigen in the early detection of prostate cancer: results of a multicenter clinical trial of 6,630 men. *J Urol* 151:1283
- Gann PH, Hennekens CH, Stampfer MJ (1995) A prospective evaluation of plasma prostate specific antigen for detection of prostatic cancer. *J Am Med Assoc* 273:289
 - Meany DL, Zhang Z, Sokoll LJ, Zhang H, Chan DW (2009) Glycoproteomics for prostate cancer detection: changes in serum PSA glycosylation patterns. *J Proteome Res* 8:613
 - Lang QL, Wang F, Yin L, Liu MJ, Petrenko VA, Liu AH (2014) Specific probe selection from landscape phage display library and its application in enzyme-linked immunosorbent assay of free prostate-specific antigen. *Anal Chem* 86:2767
 - Graves HC, Wehner N, Stamey TA (1992) Ultrasensitive radioimmunoassay of prostate-specific antigen. *Clinic Chem* 38:735
 - Oh SW, Kim YM, Kim HJ, Kim SJ, Cho JS, Choi E (2009) Point-of-care fluorescence immunoassay for prostate specific antigen. *Clin Chim Acta* 406:18
 - Hutchinson RW, Ma RL, McLeod CW, Milford-Ward A, Lee D (2004) Immunoassay with FI-ICP-MS detection-Measurement of free and total prostate specific antigen in human serum. *Can J Anal Sci Spectrosc* 49:429
 - Barbero G, Destefanis P, Procida S, Mandili G, Ulliers D, Ceruti C, Fiori C, Maule MM, Fontana D, Giribaldi G (2008) Highly specific detection of prostate-specific antigen-positive cells in the blood of patients with prostate cancer or benign prostatic hyperplasia, using a real-time reverse-transcription-polymerase chain reaction method with improved sensitivity. *BJU Int* 102:1566
 - Wan Y, Deng WP, Su Y, Zhu XH, Peng C, Hu HY, Peng HZ, Song SP, Fan CH (2011) Carbon nanotube-based ultrasensitive multiplexing electrochemical immunosensor for cancer biomarkers. *Biosens Bioelectron* 30:3093
 - Ghindilis A, Atanasov P, Wilkins M, Wilkins E (1998) Immunosensors: electrochemical sensing and other engineering approaches. *Biosens Bioelectron* 13:113
 - Warsinke A, Benkert A, Scheller FW (2000) Electrochemical immunoassays. *Fresenius J Anal Chem* 366:622
 - Pandey B, Demchenko AV, Stine KJ (2012) Nanoporous gold as a solid support for protein immobilization and development of an electrochemical immunoassay for prostate specific antigen and carcinoembryonic antigen. *Microchim Acta* 179:71
 - Salimi A, Kavosi B, Fathi F, Hallaj R (2013) Highly sensitive immunosensing of prostate-specific antigen based on ionic liquid-carbon nanotubes modified electrode: Application as cancer biomarker for prostatebiopsies. *Biosens Bioelectron* 42:439
 - Tian JN, Huang JL, Zhao YC, Zhao SL (2012) Electrochemical immunosensor for prostate-specific antigen using a glassy carbon electrode modified with a nanocomposite containing gold nanoparticles supported with starch-functionalized multi-walled carbon nanotubes. *Microchim Acta* 178:81
 - Poon CY, Chan HM, Li HW (2014) Direct detection of prostate specific antigen by darkfield microscopy using single immunotargeting silver nanoparticle. *Sensors Actuators B Chem* 190:737
 - Peng J, Zhu YD, Li XH, Jiang LP, Abdel-Halim ES, Zhu JJ (2014) Electrochemical immunoassay for the prostate specific antigen using ceria mesoporous nanospheres. *Microchim Acta* 181:1505
 - Liu B, Lu LS, Hua EH, Jiang ST, Xie GM (2012) Detection of the human prostate-specific antigen using an aptasensor with gold nanoparticles encapsulated by graphitized mesoporous carbon. *Microchim Acta* 178:163
 - Wu D, Li R, Wang HX, Liu SQ, Wang H, Wei Q, Du B (2012) Hollow mesoporous silica microspheres as sensitive labels for immunoassay of prostate-specific antigen. *Analyst* 137:608
 - Wang H, Zhang Y, Yu HQ, Wu D, Ma HM, Li H, Du B, Wei Q (2013) Label-free electrochemical immunosensor for prostate-specific antigen based on silver hybridized mesoporous silica nanoparticles. *Anal Biochem* 434:123
 - Kumar V, Srivastava S, Umrao S, Kumar R, Nath G, Sumana G, Saxena PS, Srivastava A (2014) Nanostructured palladium-reduced graphene oxide platform for high sensitive, label free detection of a cancer biomarker. *RSC Advances* 4:2267
 - Geim AK, Novoselov AK (2007) The rise of graphene. *Nat Mater* 6:183
 - Novoselov KS, Geim AK, Morozov S, Jiang D, Zhang Y, Dubonos SV, Grigorieva V, Firsov AA (2004) Electric field effect in atomically thin carbon films. *Science* 306:666
 - Novoselov KS, Jiang Z, Zhang Y, Morozov SV, Stormer HL, Zeitler U, Maan JC, Boebinger GS, Kim P, Geim AK (2007) Room-temperature quantum hall effect in graphene. *Science* 315:1379
 - Wei W, Qu X (2012) Extraordinary physical properties of functionalized graphene. *Small* 8:2138
 - Laaksonen P, Kainlahti M, Laaksonen T, Shchepetov A, Jiang H, Ahopelto J, Linder MB (2010) Interfacial engineering by proteins: exfoliation and functionalization of graphene by hydrophobins. *Angew Chem Int Edit* 49:4946
 - Shan C, Yang H, Han D, Zhang Q, Ivaska A, Niu L (2009) Water-soluble graphene covalently functionalized by biocompatible poly-L-lysine. *Langmuir* 25:12030
 - Qu Y, Ma M, Wang ZG, Zhan GQ, Li BH, Wang X, Fang HF, Zhang HJ, Li CY (2013) Sensitive amperometric biosensor for phenolic compounds based on graphene-silk peptide/tyrosinase composite nanointerface. *Biosens Bioelectron* 44:85
 - Kovtyukhova NI, Ollivier PJ, Martin BR, Mallouk TE, Chizhik SA, Buzaneva EV, Gorchinskiy AD (1999) Layer-by-Layer assembly of ultrathin composite films from micron-sized graphite oxide sheets and polycations. *Chem Mater* 11:771
 - Hummers W, Offeman R (1958) Preparation of Graphitic Oxide. *J Am Chem Soc* 80:1339
 - Du M, Yang T, Ma SY, Zhao CZ, Jiao K (2011) Ionic liquid-functionalized graphene as modifier for electrochemical and electrocatalytic improvement: comparison of different carbon electrodes. *Anal Chim Acta* 690:169